Energy 91 (2015) 102–109

Contents lists available at ScienceDirect

Energy

journal homepage: www.elsevier.com/locate/energy

# Effect of pressure on the blow-off limits of premixed $CH_4$/air flames in a mesoscale cavity-combustor

Jianlong Wan, Aiwu Fan*, Hong Yao, Wei Liu

*State Key Laboratory of Coal Combustion, Huazhong University of Science and Technology, Wuhan 430074, China*

ARTICLE INFO

*Article history:*
Received 1 May 2015
Received in revised form
5 August 2015
Accepted 13 August 2015
Available online 3 September 2015

*Keywords:*
Mesoscale combustor
Cavity
Elevated pressure
Blow-off limit
Reaction rate
Stretching effect

ABSTRACT

The blow-off limits of $CH_4$/air flames in a mesoscale cavity-combustor under various pressures (P = 1.0 −3.0 atm) are investigated numerically. The results show that the flame blow-off limit increases first and then decreases with an increasing pressure. Three typical pressures (P = 1, 2 and 3 atm) are selected to perform numerical analysis with a detailed reaction mechanism. The analysis demonstrates that the reaction intensity in the cavity is enhanced as the pressure is raised, which is beneficial for flame stability. On the other hand, the flame front is prolonged at a higher pressure. This leads to more intense stretching effect, which is detrimental for flame stability. Therefore, the flame blow-off limit depends on the competition between the positive and negative sides. When the pressure is increased from 1 atm to 2 atm, the enhancement of anchoring ability in the cavity overwhelms the augmentation of stretching effect, which leads to an increase in flame blow-off limit. However, as the pressure is further raised from 2 atm to 3 atm, the stretching effect becomes the dominated side, which results in a decrease in flame blow-off limit. In summary, these complicated interactions determine that the flame blow-off limit is a non-monotonic function of the pressure.



## 1. Introduction

With the rapid development of MEMS (micro-electro-mechanical systems) technology, the demand for micro power generation devices becomes more and more urgent. Currently, the primary power sources for portable electronics are conventional electrochemical batteries. However, the batteries have disadvantages including a short life span, a long recharging period and a low energy density. Micro-power-MEMS are considered to be promising alternatives due to their much higher energy densities [1,2]. However, there exist some challenges to maintain a stable combustion in micro- and meso-scale combustors. First, the large surface-area-to-volume ratio leads to a considerable increase in the heat-loss ratio as the combustor is scaled down. Moreover, the residence time of the gaseous mixture flowing through the combustor is very short, which sometimes makes it hard to achieve a complete combustion for the fuel [2]. Due to those problems, various unstable flames occur in small combustors [3–5]. Hence, it is vital to develop flame stabilization technologies for those miniature combustors.

By far, many methods have been used to promote the flame stability in micro- and meso-scale combustors. Heat management is a frequently applied strategy [6–11]. To name a few, Kuo and Ronney [9] studied the combustion characteristics in micro "Swiss-roll" combustors, and the results showed that a better heat recirculation effect can extend the operational limit of inlet velocity more effectively. Jiang et al. [10] proposed a miniature combustor with a porous wall that can enhance the flame stability by reducing the heat loss and the preheating effect on the fresh mixture. Wang et al. [11] pointed out that the inert porous media can significantly extend the operating range of gas flow rate and equivalence ratio of $CH_4$/air mixture. Moreover, the catalytic combustion is a good way to stabilize flame under small scales. Chen et al. [12] investigated the catalytic combustion of $H_2$/air mixture in a micro combustor, which demonstrated that the flame stability can be significantly improved by the catalyst. Choi et al. [13] confirmed that combustion can occur in a catalytic combustor of sub-millimeter scale. Baigmohammadi et al. [14,15] numerically studied the impacts of wire insertion on premixed $CH_4$/air flame and catalytic segmented bluff body on $CH_4$/H2/air flame in a micro combustor, respectively. Their results show that the inserted wire and catalytic segmented

* Corresponding author. 1037 Luoyu Road, Wuhan 430074, China. Tel.: +86 27 87542618; fax: +86 27 87540724.
*E-mail addresses:* faw@hust.edu.cn, faw_73@163.com (A. Fan).

http://dx.doi.org/10.1016/j.energy.2015.08.026
0360-5442/

bluff body have significant effects on flame stabilization and can also modify the flame location within the micro combustor.

Forming a recirculation zone or low-velocity zone in the flow field is another effective way to stabilize the flame in micro-combustors. Yang et al. [16] investigated the flame stability in micro combustors with one backward facing step. They found that the flame can remain stable in different combustor configurations over wide ranges of inlet velocity and equivalence ratio. Khandelwal et al. [17] experimentally studied the flame stabilization in a micro combustor with three steps, and the flame can be anchored with improved flammability limits. Wan et al. [18] and Fan et al. [19] developed micro bluff-body combustors that can expand the blow-off limit by several times compared with the straight channel. Recently, Wan et al. [20–22] and Yang et al. [23] studied the combustion characteristics of $H_2$/air mixtures in micro combustors with wall cavities. They found that although the flame blow-off is greatly extended by the cavity, the "flame tip opening phenomenon" occurred at relatively high velocity which leads to a sharp drop in the combustion efficiency.

Very recently, Wan et al. [24] investigated the flame behaviors of $CH_4$/air flames in a mesoscale channel with cavities experimentally and numerically. The flame blow-off limits of this cavity-combustor are several times the corresponding burning velocities of incoming mixtures, indicating that the cavities have a strong ability to extend the operational range of inlet velocity. They also investigated the effect of channel gap distance on the flame blow-off limit [25] and a monotonic dependence was found. Moreover, the impact of wall thermal conductivity was examined and they revealed a non-monotonic tendency [26]. Those findings provide a guideline for an optimum design of this type of micro- and meso-scale combustor. It is well known that the pressure has a significant effect on combustion characteristics. In the present work, we numerically investigated the flame blow-off limits of a mesoscale cavity-combustor at normal and elevated pressures. A non-monotonic variation trend of the flame blow-off limit versus the pressure was found and analyzed.

## 2. Numerical method

### 2.1. Geometric model

Fig. 1 shows the schematic of the mesoscale combustor with cavities. The width ($W_0$), height ($W_1$) and length ($L_0$) of the channel are

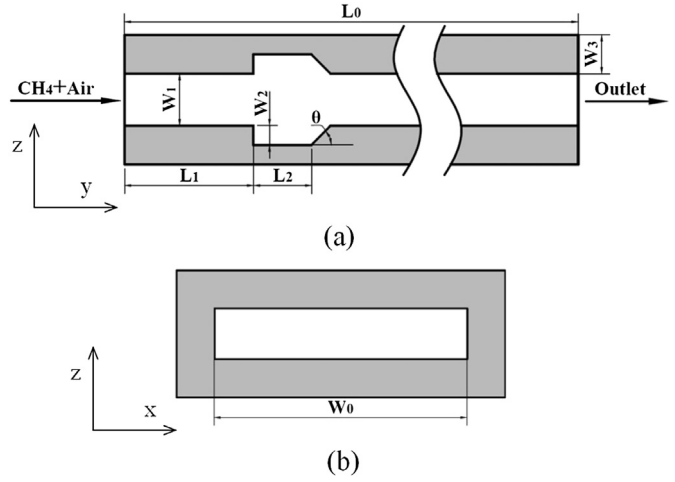


**Fig. 1.** Schematic of the mesoscale combustor with cavities: (a) longitudinal cross section, (b) vertical cross section. The origin of coordinates is located at the center of the combustor.

20 mm, 4 mm and 70 mm respectively, while the wall thickness ($W_3$) is 3 mm. The cavity length ($L_2$) and depth ($W_2$) are 4.5 mm and 1.5 mm, respectively. The angle of the ramped cavity wall ($\theta$) is set as 45°. The distance from the combustor entrance to the vertical cavity wall ($L_1$) is 10 mm. The solid material of combustor walls is quartz glass.

### 2.2. Mathematical model

First, the value of the Knudsen number, $K_n = L_g/L_c$, was estimated, where $L_g$ is the mean free path of gas and $L_c$ is the characteristic scale of the combustor. The calculation shows that the order of magnitude of $K_n$ is $10^{-5}$ for $CH_4$ and $O_2$, which is much less than the criterion of $10^{-3}$. Thus, the mixture can be reasonably regarded as a continuum and the Navier–Stokes equations are suitable for the present study [27]. As the largest Reynolds number of the incoming mixture is approximately 1,750, a three-dimensional, unsteady laminar model was adopted. The governing equations for the mixture are shown below,

Continuity:

$$\frac{\partial \rho}{\partial t} + \frac{\partial}{\partial x}(\rho v_x) + \frac{\partial}{\partial y}(\rho v_y) + \frac{\partial}{\partial z}(\rho v_z) = 0 \tag{1}$$

Momentum:

$$\text{X direction}: \frac{\partial(\rho v_x)}{\partial t} = -\left[\frac{\partial(\rho v_x v_x)}{\partial x} + \frac{\partial(\rho v_x v_y)}{\partial y} + \frac{\partial(\rho v_x v_z)}{\partial z}\right] - \frac{\partial p}{\partial x} + \frac{\partial \tau_{xx}}{\partial x} + \frac{\partial \tau_{xy}}{\partial y} + \frac{\partial \tau_{xz}}{\partial z} \tag{2}$$

$$\text{Y direction}: \frac{\partial(\rho v_y)}{\partial t} = -\left[\frac{\partial(\rho v_y v_x)}{\partial x} + \frac{\partial(\rho v_y v_y)}{\partial y} + \frac{\partial(\rho v_y v_z)}{\partial z}\right] - \frac{\partial p}{\partial y} + \frac{\partial \tau_{yx}}{\partial x} + \frac{\partial \tau_{yy}}{\partial y} + \frac{\partial \tau_{yz}}{\partial z} \tag{3}$$

$$\text{Z direction}: \frac{\partial(\rho v_z)}{\partial t} = -\left[\frac{\partial(\rho v_z v_x)}{\partial x} + \frac{\partial(\rho v_z v_y)}{\partial y} + \frac{\partial(\rho v_z v_z)}{\partial z}\right] - \frac{\partial p}{\partial z} + \frac{\partial \tau_{zx}}{\partial x} + \frac{\partial \tau_{zy}}{\partial y} + \frac{\partial \tau_{zz}}{\partial z} \tag{4}$$

Energy:

$$\frac{\partial(\rho c_p T)}{\partial t} + \frac{\partial(\rho v_x c_p T)}{\partial x} + \frac{\partial(\rho v_y C_p T)}{\partial y} + \frac{\partial(\rho v_z c_p T)}{\partial z} = \frac{\partial\left(\lambda_f \partial T\right)}{\partial x^2} + \frac{\partial\left(\lambda_f \partial T\right)}{\partial y^2} + \frac{\partial\left(\lambda_f \partial T\right)}{\partial z^2} + \sum_i \left[\frac{\partial}{\partial x}\left(\rho c_{p,i} T D_{m,i} \frac{\partial Y_i}{\partial x}\right) + \frac{\partial}{\partial y}\left(\rho c_{p,i} T D_{m,i} \frac{\partial Y_i}{\partial y}\right) + \frac{\partial}{\partial z}\left(\rho c_{p,i} T D_{m,i} \frac{\partial Y_i}{\partial z}\right)\right] + \sum_i h_i R_i \tag{5}$$

Species:

$$\frac{\partial(\rho Y_i)}{\partial t} + \frac{\partial(\rho Y_i v_x)}{\partial x} + \frac{\partial(\rho Y_i v_y)}{\partial y} + \frac{\partial(\rho Y_i v_z)}{\partial z} = \frac{\partial}{\partial x}\left(\rho D_{m,i} \frac{\partial Y_i}{\partial x}\right) + \frac{\partial}{\partial y}\left(\rho D_{m,i} \frac{\partial Y_i}{\partial y}\right) + \frac{\partial}{\partial z}\left(\rho D_{m,i} \frac{\partial Y_i}{\partial z}\right) + R_i \tag{6}$$